

Energy-Efficient Proactive Caching with Multipath Routing

Yantong Wang, Vasilis Friderikos

Abstract

The ever-continuing explosive growth of on-demand content requests has imposed great pressure on mobile/wireless network infrastructures. To ease congestion in the network and increase perceived user experience, caching popular content closer to the end-users can play a significant role and as such this issue received significant attention over the last few years. Additionally, energy efficiency is treated as a fundamental requirement in the design of next-generation mobile networks. However, there has been little attention to the overlapping area between energy efficiency and network caching especially when considering multipath routing. To this end, this paper proposes an energy-efficient caching with multipath routing support. The proposed scheme provides a joint anchoring of popular content into a set of potential caching nodes with optimized multi-path support whilst ensuring a balance between transmission and caching energy cost. The proposed model also considers different content delivery modes, such as multicast and unicast. Two separated Integer-Linear Programming (ILP) models are formulated for each delivery mode. To tackle the curse of dimensionality we then provide a greedy simulated annealing algorithm, which not only reduces the time complexity but also provides a competitive performance as ILP models. A wide set of numerical investigations has shown that the proposed scheme is more energy-efficient compared with other widely used approaches in caching under the premise of network resource limitation.

Index Terms

5G, Wireless Networks, Proactive Caching, Multipath Routing, Energy Consumption, Integer Linear Programming, Simulated Annealing

I. INTRODUCTION

THE enormous amount of mobile traffic, which is expected to reach more than 136 exabytes per month in 2024 [1], is creating great challenges to the current and emerging mobile network infrastructures. As an evolutionary network architecture, Information-Centric Networking (ICN) is designed to support content distribution and user mobility with in-network caching feature [2]. Compared with other caching approaches, proactive caching methods make a trade-off between storage capacity and latency, whose key aspects are related to the following type of questions: "where to cache", "what to cache", "cache dimensioning", and "content delivery" [3]. In this paper, the focus is on the location to anchor popular content and determining an efficient routing path to be employed for caching delivery. Despite the well-known benefits of mobile/wireless ICN, there are still some significant and challenging open-ended topics in this field, such as utilizing multipath routing, security and energy efficiency [4]. When addressing energy consumption, it is treated as one of the key pillars in the design of next-generation wireless networks, which is not only important in monetary terms due to energy savings but also for curbing the CO_2 emissions [5] and align operators with the goals related to the so-called 1.5-Degree-C climate trajectory¹. The energy consumption in ICN can be divided into two parts [6]–[12]: the energy required for caching content and the energy for data transmission. Content replicas can be placed near access routers as a mean of reducing transmission costs but with an extra cost paid for hosting popular content; reversely, consolidating caching host nodes can be adopted to reduce caching energy consumption at the expense of an increased transmission cost. This inherent trade-off raises the following key question: where to cache popular content and how to design an efficient routing path to minimize the total energy consumption whilst satisfying the network resource limitations.

There are a number of prior works on the issues related to location selection for hosting popular content in order to minimize energy consumption. An integer linear programming (ILP) model is studied in [6], where the limitation of router caching space and different caching hardware technologies have been considered. J. Llorca *et al.* [7] take explicitly into account the temporal and spatial dynamics of user requests and the heterogeneity of network resources. In [8], the authors present a distributed in-network caching solution, in which each content router only needs local information. An energy consumption model with propagation delay-

¹www.ipcc.ch/sr15/chapter/spm

awareness is investigated in [9] and a quantized Hopfield neural network is proposed to derive competitive solutions. The relationship between aggregate energy consumption per transmitted bit of information and the average number of hops has been studied in [10]. A hybrid caching policy for reducing latency and energy consumption is designed in [13] which consists of device local caching, device-to-device (D2D) caching, small base station (SBS) caching and macro base station (MBS) caching. Except for saving the traditional energy in the above works, energy harvesting technology together with cooperative caching have received scholarly attention in recent years, such as SBS caching [14] and D2D caching [15]. Furthermore, some studies have investigated the energy-efficient schemes by jointly considering caching, communication, and computation. For instance, the authors in [11] propose a framework combining software defined networking, caching, and computing to balance the energy consumption and network resource utilization, which has the potential to support general in-network services. The inherent lack of user request arrival knowledge case is considered in [12] where caching, transcoding, and backhaul retrieving are jointly optimized. Another joint optimization research can be found in [16] which concentrates on the trade-offs between communication, computation and caching. The authors also provide a ϵ -optimal solution to the proposed non-linear optimization model.

The majority of the above works do not take the routing policies into consideration [6], [8], [9], [12]–[15] or only adopt the shortest path [7], [10], [11], [16]. However, it is insufficient to only consider the shortest path routing especially when the network bandwidth is limited. There are also some researches discussing the routing design in caching policies. For example, the study in [17] formulates the joint caching and multipath routing problem as an ILP model to maximize the volume of caching-served file requests in the wireless network. Chu *et al.* [18] jointly consider the cache allocation and routing path to maximize content utilities based on cache partitioning. The delay optimization scenario is also considered in [18]. The authors in [19] investigate the caching and routing problem considering both source routing and nominal shortest path routing to minimize routing cost. To simplify the model, the link bandwidth in [19] is assumed to be abundant. For a more detailed and extensive treatment of the overall state-of-the-art caching and routing policies in ICN, we refer the reader to [20].

In this article, we jointly consider the caching placement and multipath routing to minimize the total energy consumption and study the following two content delivery modes [21]: 1) the service flow can be shared if the users have the same content preference as well as connected access router, which is called *multicast mode*. For example, semi-synchronous requests can be

bundled together and served via a single transmission; 2) the service flow cannot be shared and each request is satisfied with an independent transmission, i.e. *unicast mode*. We also consider explicitly the caching memory space and link bandwidth limitations. The existing research in [22] is closest to the problem we tackle here. Though [22] considers the energy-efficient caching and routing algorithm, here are some main differences between our work and [22]. On the one hand, the caching methods are quite different. For example, we allow replicated caching while [22] considers unique caching that each content is satisfied by exactly one node. On the other hand, our work includes modelling for different delivery modes, i.e. multicast and unicast, while [22] only considers the unicast case. The proposed scheme can be deployed in the control plane which can cooperate with the baseband processing units (BBU) in the software defined wireless network structure [23]. The salient contributions of this paper are summarized as follows.

- We propose an energy-efficient caching scheme by jointly considering the content placement and multipath routing, then formulate it as an optimization model with caching space and link capacity limitations. In particular, we provide two ILP models according to two delivery modes, multicast and unicast respectively.
- Since the proposed ILP models belong to the NP-hard family of problems, we provide a heuristic algorithm named Greedy Simulated Annealing Caching (GSAC). In this approach, we divide the original problem into several sub-problems and employ simulated annealing to find competitive sub-optimal caching nodes recursively.
- To understand the performance gap among evaluated methods, a wide-set of simulations is performed under different scenarios. More specifically, we evaluate influences from the aspects of the user (in terms of the number of requests, user preference and prediction accuracy) and the network (such as the available bandwidth and caching space and the underlying network topology).

The rest of this paper is organized as follows. Section II formulates the system model. Section III provides a simulated annealing-based heuristic algorithm. In the end, Section IV and V give the numerical investigations and conclusions respectively.

II. SYSTEM MODEL

A. Network Model

The network is modelled as an undirected graph $\mathcal{G} = \{\mathcal{E}, \mathcal{L}\}$ as shown in Figure 1, where \mathcal{E} represents the set of nodes and \mathcal{L} denotes the set of links. Each link $l \in \mathcal{L}$ equips with

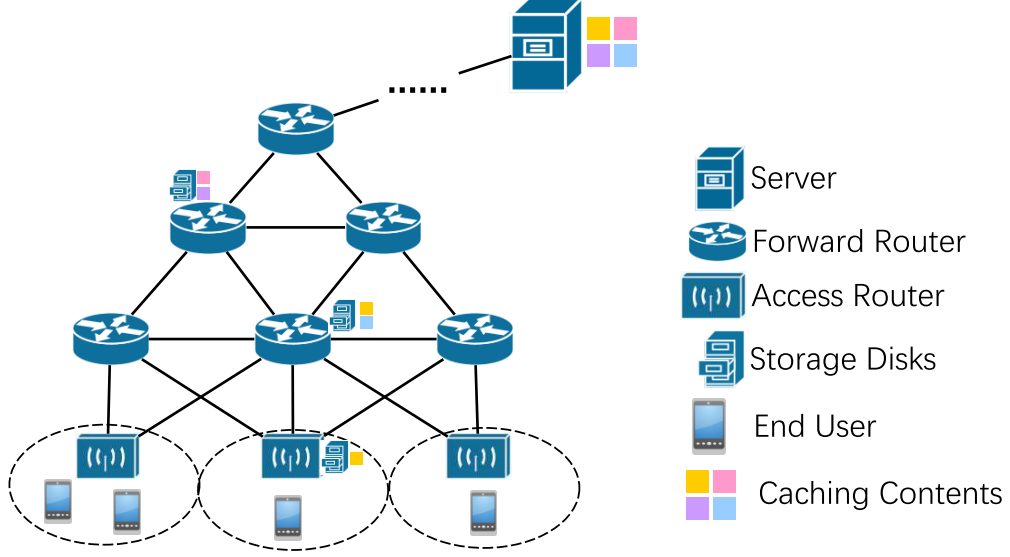


Figure 1: System Model

bandwidth c_l . The nodes are partitioned to access routers (AR) $\mathcal{A} \subset \mathcal{E}$, forward routers $\mathcal{F} \subset \mathcal{E}$ and server $\{0\} \in \mathcal{E}$. Additionally, each caching node $e \in \mathcal{E}^0 = \mathcal{E} \setminus \{0\}$ has storage capacity w_e and can provide both data flow forwarding and content caching services.

Let \mathcal{N} be the set of contents. For each content $n \in \mathcal{N}$, the required caching size and transmission bandwidth are represented by s_n and b_n respectively. Without loss of generality, we assume all contents can be fetched from the server in case of a cache miss. The user's preference is described as ρ_{kn} , which is the probability of user k requests file n . Furthermore, we use π_{ka} to represent the user k accesses to the network service via AR a , which depends on the user movement behaviour. For modelling simplification purpose, we assume the user's movement is already known thus π_{ka} becomes a binary indicator; otherwise, π_{ka} is the moving probability and the model for this case is discussed in our previous work [24]. Consequently the aggregated number of request for content n at AR a , λ_{na} , can be determined by $\lambda_{na} = \sum_k \pi_{ka} \cdot \rho_{kn}$. The used symbols and their meanings are summarized in Table I.

B. Energy Model

In this paper, we focus on two types of energy consumption in the caching-enabled network: the caching energy E^C and the communication transmission energy E^T . Therefore, the total energy consumption can be represented by $E = E^C + E^T$. Similar to [12], the caching energy is

Table I: Summary of Main Notations

Symbol	Description
\mathcal{E}^0	the set of caching candidates
\mathcal{A}	the set of access routers (AR), $A \in \mathcal{E}^0$
$\{0\}$	the data server
\mathcal{N}	the set of contents
\mathcal{E}	the set of nodes, $\mathcal{E} = \mathcal{E}^0 \cup \{0\}$
\mathcal{L}	the set of links
\mathcal{K}	the set of users
α	power efficiency of caching 1 bit data (Watts per bit)
β	power cost for transmitting 1 bit data within 1 hop (Joule per bit per hop)
T	the time interval normalization factor
s_n	the size of content n
b_n	the bandwidth requirement of content n
w_e	the available space in caching node e
c_l	the capacity of link l
ρ_{kn}	the preference on content n for user k
π_{ka}	the connection with AR a for user k
λ_{na}	the aggregated number of request for content n at AR a
N_{aep}	the number of hops for path $p \in \mathcal{P}_{ae}$
B_{laep}	indicates the link l is in path $p \in \mathcal{P}_{ae}$ or not
x_{ne}	indicates the content n is cached in node e or not
y_{naep}	indicates the delivery of content n uses path $p \in \mathcal{P}_{ae}$ or not

a proportional function of content size and can be given by,

$$E^C = \sum_{n \in \mathcal{N}} \sum_{e \in \mathcal{E}^0} \alpha \cdot s_n \cdot x_{ne} \cdot T, \quad (1)$$

where α is the power efficiency for caching 1-bit of information; s_n is the caching space for content n ; x_{ne} is a binary decision variable with,

$$x_{ne} = \begin{cases} 1, & \text{if content } n \text{ is cached in node } e; \\ 0, & \text{otherwise;} \end{cases}$$

T is the time interval normalization factor partitioned in epochs of equal length and the hosting content in one time period might be totally different from the data in the next time epoch, which is also called caching refreshing cycle [12] or windowed grouped data aggregation [16]. Without loss of generality, hereafter we focus on optimization procedures in one time epoch.

The communication transmission energy consumption is measured by the number of hops in

the network and can be given by,

$$E^T = \sum_{n \in \mathcal{N}} \sum_{a \in \mathcal{A}} \sum_{e \in \mathcal{E}} \sum_{p \in \mathcal{P}_{ae}} \beta \cdot N_{aep} \cdot s_n \cdot y_{naep}, \quad (2)$$

where β is the energy cost for transmitting 1-bit of information within a single hop; N_{aep} expresses the number of hops on path $p \in \mathcal{P}_{ae}$ and \mathcal{P}_{ae} represents all available paths between AR a and caching node e ; notably $N_{aep} = 0$ if $a = e$; y_{naep} is a decision variable with

$$y_{naep} = \begin{cases} 1, & \text{if the delivery of content } n \text{ uses path } p \in \mathcal{P}_{ae}; \\ 0, & \text{otherwise.} \end{cases}$$

It is worth noting that we do not take the static energy consumption of network devices into consideration, such as the idle power to support routers and network interfaces. In this paper, these devices are assumed to keep power-on to provide various kinds of network services for different requests, instead of only content caching.

C. Optimization Model

In this subsection, we consider two delivery modes, i.e. the multicast and the unicast mode. For modelling simplification, the following optimization models are under the assumption that the user's interested content is already known, which indicates ρ_{kn} becomes a binary indicator to bridge user k and content n . The user preference prediction has been extensively studied in the context of caching, such as [25] and [26], and this technique is beyond the scope as well as complimentary of this paper. The influence of the predicted accuracy on system energy consumption is discussed in Section IV.

1) *Multicast Mode*: The ILP model is formulated as follows:

$$(P1) \quad \min_{x_{ne}, y_{naep}} E \quad (3a)$$

$$\text{s.t.} \quad \sum_{n \in \mathcal{N}} s_n \cdot x_{ne} \leq w_e, \forall e \in \mathcal{E}^0; \quad (3b)$$

$$\sum_{n \in \mathcal{N}} \sum_{a \in \mathcal{A}} \sum_{e \in \mathcal{E}} \sum_{p \in \mathcal{P}_{ae}} b_n \cdot B_{laep} \cdot y_{naep} \leq c_l, \forall l \in \mathcal{L}; \quad (3c)$$

$$y_{naep} \leq x_{ne}, \forall n \in \mathcal{N}, a \in \mathcal{A}, e \in \mathcal{E}^0, p \in \mathcal{P}_{ae}; \quad (3d)$$

$$y_{naep} \leq \lambda_{na}, \forall n \in \mathcal{N}, a \in \mathcal{A}, e \in \mathcal{E}, p \in \mathcal{P}_{ae}; \quad (3e)$$

$$\lambda_{na} \cdot \sum_{e \in \mathcal{E}} \sum_{p \in \mathcal{P}_{ae}} y_{naep} = \lambda_{na}, \forall n \in \mathcal{N}, a \in \mathcal{A}; \quad (3f)$$

$$x_{ne} \in \{0, 1\}, \forall n \in \mathcal{N}, e \in \mathcal{E}^0; \quad (3g)$$

$$y_{naep} \in \{0, 1\}, \forall n \in \mathcal{N}, a \in \mathcal{A}, e \in \mathcal{E}, p \in \mathcal{P}_{ae}. \quad (3h)$$

The objective function (3a) aims to minimize the total energy consumption, which is introduced in subsection II-B. Constraint (3b) relates to the storage space used for caching which should not exceed the node capacity. Constraint (3c) satisfies the link bandwidth limitation. We note that B_{laep} is a binary indicator, where $B_{laep} = 1$ means the link l is in path $p \in \mathcal{P}_{ae}$, and $B_{laep} = 0$, otherwise. Therefore, $\sum_a \sum_e \sum_p B_{laep} \cdot y_{naep}$ selects all links used for content n delivery. Constraint (3d) limits the source of delivery path should host related contents. Moreover, in constraint (3e) when $\lambda_{na} = 0$, y_{naep} is forced to be 0, which means the delivery path to AR a should not be assigned if there is no such content requirement in that AR; and in constraint (3f) if $\lambda_{na} \neq 0$, $\sum_e \sum_p y_{naep} = 1$ indicating that when there is content requirement in AR a we must allocate a delivery path accordingly. It is worth noticing that when dealing with caching allocation, we only focus on the storage node $e \in \mathcal{E}^0$ such as constraints (3b) and (3d); however, for the path assignment, we consider both the caching node $e \in \mathcal{E}^0$ (for cache hitting case) and the core network server $\{0\}$ (for cache missing case), like constraint (3c), (3e) and (3f).

2) *Unicast Mode*: In this case, y_{naep} is no longer binary but an integer decision variable where the value represents the number of flows for content n that traverse path $p \in \mathcal{P}_{ae}$. In that case, the proposed ILP model would be as follows,

$$(P2) \quad \min_{x_{ne}, y_{naep}} \quad (3a) \quad (4a)$$

$$\text{s.t.} \quad y_{naep} \leq M \cdot x_{ne}, \forall n \in \mathcal{N}, a \in \mathcal{A}, e \in \mathcal{E}^0, p \in \mathcal{P}_{ae}; \quad (4b)$$

$$\sum_{e \in \mathcal{E}} \sum_{p \in \mathcal{P}_{ae}} y_{naep} = \lambda_{na}, \forall n \in \mathcal{N}, a \in \mathcal{A}; \quad (4c)$$

$$y_{naep} \in \mathbb{Z}^{0+}, \forall n \in \mathcal{N}, a \in \mathcal{A}, e \in \mathcal{E}, p \in \mathcal{P}_{ae}; \quad (4d)$$

$$(3b), (3c), (3g).$$

The constraint (4b) updates from constraint (3d) and M is a sufficiently large number, which represents this node can serve infinite requests as long as it hosts the required content. For the scenario considering node service capability, M should be replaced by the service rate, i.e. the

number of requests that a node can serve during the time period T , which is discussed in [24]. Constraint (4c) replaces constraint (3e) and (3f), where all served flows for content n at AR a should exactly match the number of requests.

III. HEURISTIC ALGORITHM

The ILP models (P1) and (P2) belong to the family of NP-hard problems. The proof can be given by reduction from the uncapacitated facility location (UFL) problem, via setting $s_w = c_l = +\infty$; note that the UFL is a well-known NP-hard problem. To solve (P1) and (P2) in a pseudo real-time manner, we propose a Greedy Simulated Annealing Caching (GSAC) algorithm. In GSAC, the original optimization model is decomposed by the content categories and these contents are allocated in descending order, i.e. the network serves the content with the most requests first. Then, for each content assignment, we employ a simulated annealing algorithm to allocate popular content in the most suitable nodes.

Simulated Annealing (SA) is a well-known optimization method for approximating the global optimal solution. The main structure of SA contains two nested loops, where the external is controlled by the temperature and the internal is managed by a Markov-chain length. In each loop a new solution is produced and compared with the previously stored result; the new solution is accepted if its performance is better; otherwise, it would be accepted with some predefined probability. The iterations continue until meeting the stopping criterion.

Regarding the optimization model (P1), the solution generated in each loop includes the decision variable x_e and y_{aep} (here we deal with the sub-problem oriented towards specific content n , so n is omitted from the subscript notation for simplification). Note, however, that the decision about those two variables, i.e., x_e and y_{aep} , might result in an infeasible allocation. To restore feasibility, we set x_e as the pivot variable. Then, once x_e is allocated, y_{aep} can be determined as follows,

$$\begin{cases} y_{a\{0\}1} = 1, & \text{if } \sum_{e \in \mathcal{E}^0} x_e = 0 \text{ and } \{a | \lambda_a > 0\}; \\ y_{aep} = 1, & \text{if } \{(a, e, p) | \lambda_a > 0, x_e = 1, \min N_{ae1}, b \leq c_l, \forall a \in \mathcal{A}, e \in \mathcal{E}^0, l \in p \in \mathcal{P}_{ae}\}; \\ y_{aep} = 0, & \text{otherwise.} \end{cases} \quad (5)$$

When there is caching miss ($\sum_{e \in \mathcal{E}^0} x_e = 0$), the request is redirected to the server $\{0\}$; when some nodes host the content, the delivery path is from the requesting AR ($\lambda_a > 0$) to the nearest

caching node ($\min N_{ae1}, x_e = 1$). Additionally, the link bandwidth constraint is also considered in routing by setting $b \leq c_l$; otherwise, $y_{aep} = 0$.

The determination of y_{aep} in problem (P2) is similar to (5):

$$\begin{cases} y_{a\{0\}1} = \lambda_a, & \text{if } \sum_{e \in \mathcal{E}^0} x_e = 0 \text{ and } \{a | \lambda_a > 0\}; \\ y_{aep} = \lfloor \frac{c_l}{b} \rfloor, & \text{if } \{(a, e, p) | \lambda_a > 0, x_e = 1, \min N_{ae1}, b \leq c_l, \forall a \in \mathcal{A}, e \in \mathcal{E}^0, l \in p \in \mathcal{P}_{ae}\}; \\ y_{aep} = 0, & \text{otherwise.} \end{cases} \quad (6)$$

It is worth noting at this point that when some nodes host the content, we keep allocating content delivery by $y_{aep} = \lfloor \frac{c_l}{b} \rfloor$ until $\sum_{e \in \mathcal{E}^0} \sum_{p \in \mathcal{P}_{ae}} y_{aep} = \lambda_a$.

The details of the GSAC is depicted in Algorithm 1. There are four hyperparameters involved as explained in the sequel. The L parameter controls the internal loop, whilst parameters T_0 , T_{end} and γ manage the external loop. Moreover, the current temperature influences the acceptance probability, i.e. the exploration of searching space. The configuration of these values depends on the scope of the problem. In this paper, after several rounds of grid search and by considering the trade-off between time complexity and performance, the best configuration is recorded as follows: $T_0 = 10^3$, $T_{end} = 10^{-3}$, $\gamma = 0.8$ and $L = 200$.

IV. NUMERICAL INVESTIGATIONS

A. Simulation Setting

In this section, we compare the caching allocation derived from the set of proposed schemes against a simple but powerful solution which we call Random Caching and the Greedy Caching technique which has been proposed in [24]. The proposed set of techniques include the ILP optimization model (which is viewed as the optimal solution in this paper, hence in the following figures we use the term Optimal to represent the result of ILP model) and the GSAC technique. Random Caching can be deemed as a technique that can be easily adopted and used by operators where hosting nodes are chosen randomly for the requested content. The Greedy Caching allocates the nearest node packing the requested content for a specific user if there is sufficient caching space. The performance is evaluated via two metrics: the energy gain and cache-hit ratio. As for the energy gain, we use the so-called No-caching approach as the benchmark, which in essence means that we do not host any content in caching nodes and each flow request should be transferred to the core network content server for the information; and the gain is calculated

Algorithm 1: Greedy Simulated Annealing Caching (GSAC) Algorithm

Data: Variables in Table I;

Simulated Annealing Initial Temperature T_0 ;

Stopping Temperature T_{end} ;

Annealing Parameter γ ;

Markov-chain Length L

Result: Cache allocation x_{ne} and path delivery y_{naep}

```

1 Initialize  $\mathcal{N}' = \{n | \sum_{a \in \mathcal{A}} \lambda_{na} > 0\}$  and sort descendingly;
2 Generate  $\{p | p \in \mathcal{P}_{ae}\}$  the k-shortest path for each  $(a, e)$  pair via Yen's Algorithm;
3 foreach  $n \in \mathcal{N}'$  do // Simulated Annealing
4   Initialize  $x_e$  randomly satisfying  $\{x_e \in \{0, 1\} | s_n \leq w_e, \forall e \in \mathcal{E}^0\}$ ,  $T \leftarrow T_0$ ,  $k \leftarrow 1$ ;
5   Determine  $y_{aep}$  through (5) or (6); // for (P1) and (P2) respectively
6   Set best solution  $x^*, y^* \leftarrow x_e, y_{aep}$ ;
7   while  $T \geq T_{end}$  do
8     while  $k \leq L$  do
9       Generate  $x'_e$  via flipping one bit in  $x_e$  randomly;
10      Determine  $y'_{aep}$  through (5) or (6);
11      if  $\delta = E(x'_e, y'_{aep}) - E(x_e, y_{aep}) < 0$  then
12        Update  $x_e, y_{aep} \leftarrow x'_e, y'_{aep}$ ;
13        if  $E(x'_e, y'_{aep}) - E(x^*, y^*) < 0$  then
14          Update  $x^*, y^* \leftarrow x'_e, y'_{aep}$ ;
15        end
16      else
17        Update  $x_e, y_{aep} \leftarrow x'_e, y'_{aep}$  with probability  $\exp(-\delta/T)$ ;
18      end
19       $k \leftarrow k + 1$ ;
20    end
21     $T \leftarrow \gamma \times T$ ;
22  end
23   $x_{ne}, y_{naep} \leftarrow x^*, y^*$ ;
24  Update  $w_e, c_l$ ;
25 end

```

by the energy of No-caching over the energy of evaluated algorithm. Regarding the cache-hit ratio, it is defined as the percentage of content requests served by caching nodes.

The experiments are performed in a 10-node 16-link network model, which captures a nominal tree-like configuration of a mobile network. We assume that all links have equal capacity and all caching nodes have identical memory space, but the value varies to investigate the trade-off between bandwidth and memory (caching capacity). Additionally, we assume that the content requests follow the typically used 80/20 rule, i.e. the majority of predictions focus on 20% of the content categories. The caching allocation is based on such prediction and the impact of predicted

accuracy is also discussed. All results presented hereafter are averaged over one hundred Monte Carlo iterations and based on those we analyse the performance of the different schemes. To put the computational times in perspective simulations performed using MATLAB R2021a running on top of a 64-bit Ubuntu 20.04.2 LTS environment, whilst the machine is equipped with an Intel Core i7-6700HQ CPU with 32GB RAM. The simulation parameters assumed in the investigations are presented and summarized in Table II. Unless stated otherwise, the value of w_e , c_l , ρ_{kn} , and $\sum_a \lambda_{na}$ are set as the default.

Table II: Simulation Parameters [27]

Parameter	Default Value	Range
caching power coefficient (α)	2.5×10^{-9} W/b	-
transmitting energy coefficient (β)	4×10^{-8} J/b	-
content categories ($ \mathcal{N} $)	100	-
content size (s_n)	-	[10,100] MB
content transmitting bandwidth (b_n)	-	[10,100] Mbps
available caching space (w_e)	0.5GB	[0.25,1] GB
available link capacity (c_l)	0.5Gbps	[0.25,1] Gbps
preference prediction accuracy (ρ_{kn})	100%	[0%,100%]
number of requests ($\sum_a \lambda_{na}$)	100	[20,160]
time slot duration (T)	10 s	-

B. Impact of the Number of Requests

We first study how the number of content requests affects the performance of the proposed schemes, where we set $\sum_a \lambda_{na}$ from 20 to 160. In Figure 2.(a), both the optimal and GSAC on (P1) share a climbing-remaining-dropping trend while the random keeps falling down. With the user requests' increment, and as expected, the energy consumption for caching service is increasing accordingly, and this trend is independent if we utilize the optimal scheme, the GSAC, the Greedy, the Random, or the No-caching. However, the increasing rate plays a significant role in the overall energy gains: 1) the climbing (positive slope) represents the No-caching grows at a faster rate than the evaluated algorithm; 2) the remaining (zero slope) shows that both the No-caching and the evaluated algorithm have similar increasing rate; 3) the dropping (negative slope) indicates that the No-caching grows slower than the evaluated algorithm. In Figure 2.(a), when the number of requests ranges from 20 to 60, the network has sufficient resources (i.e. caching space and link bandwidth) to serve end-users, and the optimal together with GSAC

can both significantly outperform the No-caching scheme in reducing energy consumption. The energy gain ranges from 3.44 to 4.23 for the optimal, 3.13 to 3.87 for GSAC. Then, the network becomes saturated when the number of requests ranges between 60 and 120, which reflects as a steady curve on the energy gain. After 120 requests, more users' flows are redirected to the server, and therefore the energy consumption of the optimal and GSAC grows faster than the No-caching. Hence the energy gain is reduced to 3.94 for the optimal and 3.50 for GSAC. Regarding Greedy Caching, the energy gain fluctuates between 2.70 and 3.01 according to the number of requests. Since it endeavours to assign the requested content to the nearest node, Greedy Caching provides saving in the transmission energy but pays more for hosting the contents. For Random Caching, there has been a gradual decline from 2.58 to 1.88 in the simulation, which indicates this method cannot deal with the increasing requests flexibly. It is worth noting that the energy gain in Figure 2.(a) is above 1, so all evaluated algorithm can save energy compared to the No-Caching approach. Figure 2.(b) reveals that there has been a continuous decrease in cache-hit ratio with the number of requests increment. Generally, the optimal, GSAC and Greedy guarantee the majority of requests (over 95% in the simulation) can be satisfied on the caching nodes, while nearly a third of the flows are redirected to the server in Random Caching 160-request case. Particularly, the ratio of optimal and GSAC has a marked decrease after 120 requests, which matches the turning points in Figure 2.(a).

A similar pattern still holds on (*P2*) as shown in Figure 2.(c) and 2.(d). However, in this case now the energy gain of the optimal keeps rising beyond the 120 requests. The reason is that in (*P2*) each flow is served independently, even if the requested content is in essence the same. Thus the No-caching algorithm consumes much more energy than (*P1*). Although the optimal energy is also increasing, it is at a slower rate than the No-caching which reflects a positive slope when the number of requests ranges from 120 to 140. After 120 requests, the performance gap between GSAC and Greedy in Figure 2.(c) gets smaller. In contrast to the dropping in 2.(a), the lack of more generalized hyperparameters of GSAC should be blamed instead of network resource limitation. Because the optimal solution keeps increasing which indicates the better allocation exists but GSAC cannot find it. What is interesting in (*P1*) and (*P2*) is the influence of delivery mode on energy gain and cache-hit ratio: on the one hand, unicast mode (*P2*) generates more traffic flows which make the energy gain higher than (*P1*) by comparing Figure 2.(a) and 2.(c) vertically; on the other hand, more flows exhaust the network resource rapidly and thus the cache-hit ratio in 2.(d) is less than 2.(b).

The running time of ($P1$) and ($P2$) are evaluated in Figure 2.(e) and 2.(f) respectively. The time for optimal solution varies from 6.80 seconds to around 13 minutes, while the proposed heuristic algorithm GSAC is less than 400 milliseconds and the Greedy as well as Random are less than 10 milliseconds.

In Figure 2, the optimal outperforms the other methods in both ($P1$) and ($P2$) problems, albeit with a higher time complexity cost. The heuristic method GSAC is able to provide a competitive result, followed by Greedy and Random. For instance, in ($P1$) GSAC saves 99.8% running time with the cost of approximate 7.9% performance loss when there are 100 requests. Under the same scenario, the time-saving ratio for Greedy Caching and Random Caching is 99.9% compared with the optimal solution; but the performance reductions are 33.1% and 50.7% respectively.

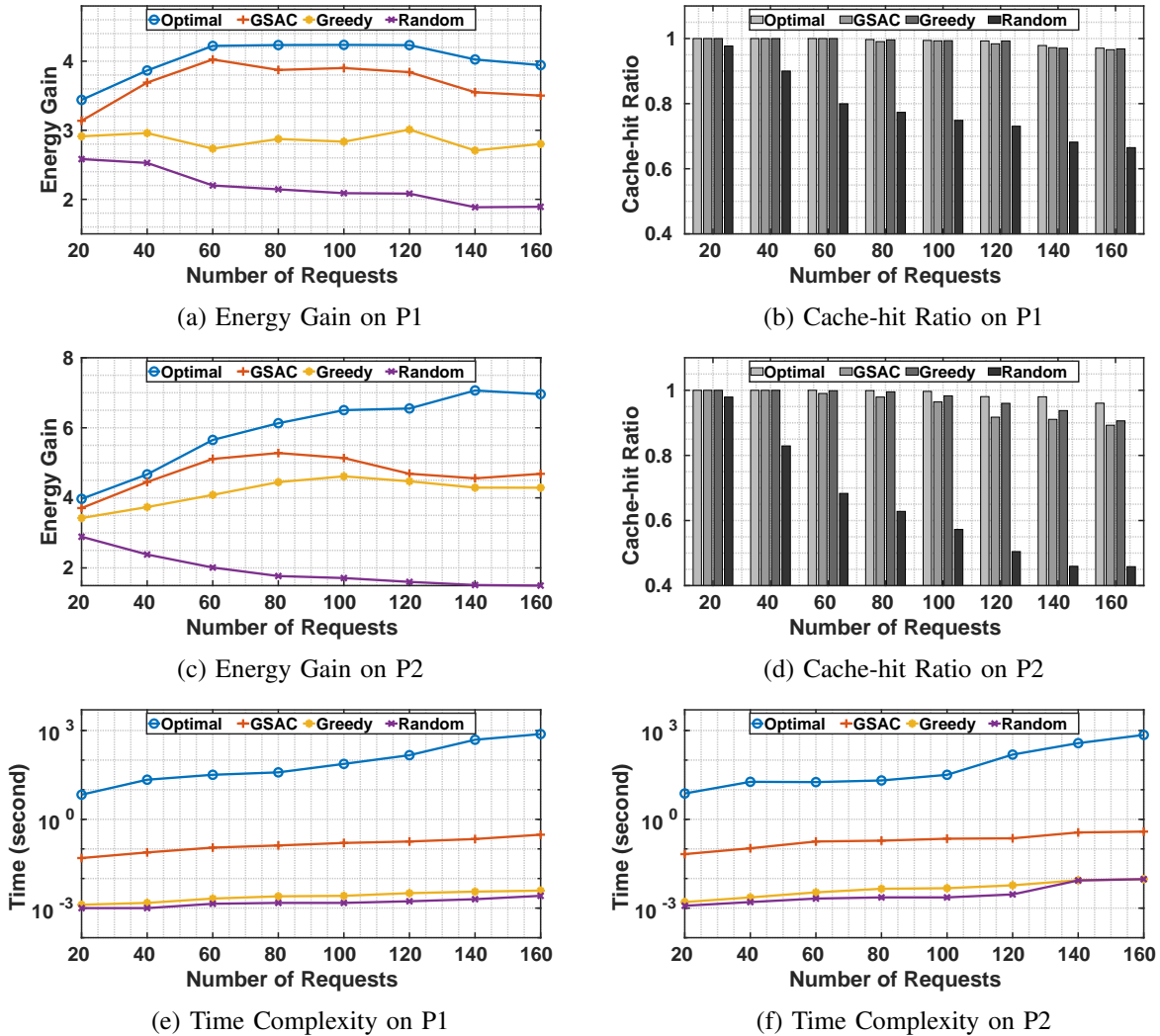


Figure 2: Algorithms Performance versus the Number of Requests

C. Impact of the Network Capacity (bandwidth & space)

To understand the trade-off between the bandwidth and caching space, the values of the parameters w_e and c_l are varied from 0.25 to 1 with a sampling interval of 0.25. This setting tries to shed light on the following question: when the memory space and link capacity are insufficient to support all content requests, to further improve the performance (i.e. energy gain and cache-hit ratio), should we increase the link capacity first or the caching space?

In Figure 3 we test the performance of different algorithms on $(P1)$ and $(P2)$. The contour lines with labels represent the energy gain or cache-hit ratio accordingly. Moreover, the blue arrows show the gradient, which can be viewed as the optimized directions. In Figure 3.(a), when both the bandwidth and memory are less than 0.5, either increasing the caching space or expanding the link capacity results in the energy gain growth. Once the memory space is larger than 0.5GB, the benefit from expanding link bandwidth is greater than memory, as shown in Figure 3.(a) that the arrow points towards the bandwidth increasing direction. To some extent, enlarging the caching memory implies more energy consumption for hosting content. A similar trend holds on Figure 3.(b), 0.5GB works as a watershed: before 0.5GB both bandwidth and caching memory make contributions to the energy gain; after 0.5GB the bandwidth dominates the performance improvement. Regarding Greedy Caching in Figure 3.(c), when the bandwidth is above 0.5Gbps, enlarging the caching space can bring more benefits compared with link capacity increasing, as the arrow points the vertical direction. The main reason for its insensitivity on link capacity is that when the memory space is sufficient, Greedy Caching allocates the content replicates in the nearest node, which is the access router in most cases. Therefore, each request can be severed locally and do not occupy any bandwidth resource. When it comes to $(P2)$, the tendencies of optimal 3.(i), GSAC 3.(j) and Greedy 3.(k) are similar with $(P1)$. What is striking in Figure 3.(d) is that all arrows point towards the bandwidth increasing direction, which indicates that an expanding link capacity has a distinct effect on the energy gain improvement while the caching space seems of not significantly contributing. Additionally, from Figure 3.(h), 3.(l), and 3.(p), the performance of Random Caching is very sensitive to the bandwidth change but sluggish to the caching memory. For the other cases of cache-hit ratio, both caching space and link bandwidth play an equally important role in the performance improvement, as the slope of arrows almost keeps close to 1.

Thus, the answer on how to prioritize expanding of the caching memory first or the link

capacity can be categorized into 3 cases: 1) for the optimal and GSAC algorithms, both bandwidth and memory expanding lead to better cache-hit ratio. However, raising the link capacity can bring more energy gains, especially when the memory space exceeds 0.5GB on (*P1*) or 0.75GB on (*P2*); 2) regarding Greedy Caching, the cache-hit ratio is affected by both bandwidth and memory space. Nevertheless, the caching memory plays a dominant factor in energy gains for capacities larger than 0.5Gbps; 3) for the Random Caching, increasing the bandwidth produces obvious benefits.

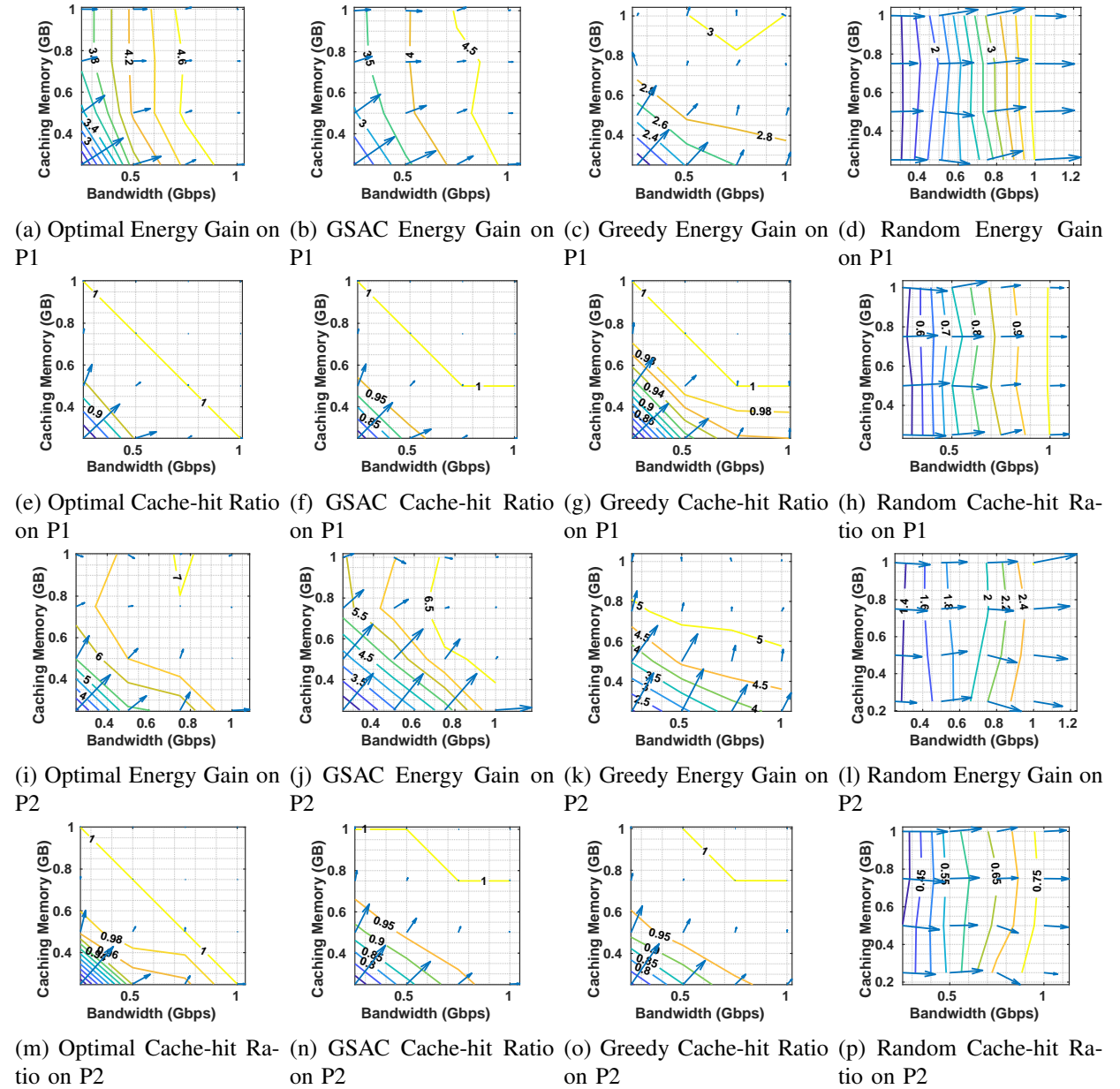


Figure 3: The Trade-off between Bandwidth and Caching Space

D. Impact of the Network Topology

The influence of different topologies is investigated in Table III. In addition to the tree-like network used in the previous simulations which is marked as original, we also employ a tree structure where other nodes cannot be reached except through the root, and a full mesh topology that each pair of nodes is connected via a direct link. It is expected that as the degree of a node in the network increases, both the energy gain and cache-hit ratio of the evaluated algorithms can be further improved since providing more direct connections is equivalent to expanding the available link bandwidth, especially for (P2). It is also clearly illustrated that in the full mesh network, even Random Caching can be considered as a comprehensive method for energy-saving purpose. But the Greedy Caching underperforms because the caching energy dominates the total energy consumption while its advantage on saving transmission energy becomes less obvious in full mesh network particularly.

Table III: Algorithms Performance versus Network Topology

		P1			P2		
Topology		Tree	Original	Full Mesh	Tree	Original	Full Mesh
# Nodes		10	10	10	10	10	10
# Links		9	16	45	9	16	45
Energy Gain	Optimal	3.77	4.24	6.22	6.16	6.50	9.79
	GSAC	3.39	3.90	6.07	4.59	5.14	9.13
	Greedy	2.82	2.83	3.35	4.37	4.61	5.66
	Random	1.65	2.09	5.76	1.45	1.71	7.56
Cache-hit Ratio	Optimal	0.99	0.99	1.00	0.99	0.99	1.00
	GSAC	0.97	0.99	1.00	0.94	0.96	1.00
	Greedy	0.99	0.99	1.00	0.97	0.98	1.00
	Random	0.62	0.75	1.00	0.46	0.57	1.00

E. Impact of the Prediction Accuracy (ρ_{kn})

In the previous evaluation, we test the performance under an ideal condition that all users' preference is exactly predicted, i.e. $\rho_{kn} = 1$. Hereafter, we relax this assumption and perform experiments to understand the impact of prediction accuracy by varying it from 100% to 0%. As shown in Figure 4.(a) and 4.(c), regarding the optimal, GSAC, and Greedy Caching, there has been a steep drop on the energy gain from 100% to 80% then the value decline steadily.

Meantime, the performance gap among the optimal, GSAC, Greedy, and Random Caching becomes very small. It is worth noting that for ($P1$), when the predicted accuracy is less than 30% (For ($P2$), the threshold is 10%), the energy gain is less than 1. In other words, the proactive caching method cannot save energy but consume more than No-caching if the user preference prediction is inaccurate since we pay extra energy for caching contents. In Figure 4.(b) and 4.(d), the cache-hit ratio reduces along with the accuracy declining. An interesting fact is that even the prediction accuracy reduces to 0%, the cache-hit ratio is still above 0. The main reason is that inaccurately predicted request can be redirected to other nodes where the required content is cached, and it is still counted for the cache-hit ratio calculation.

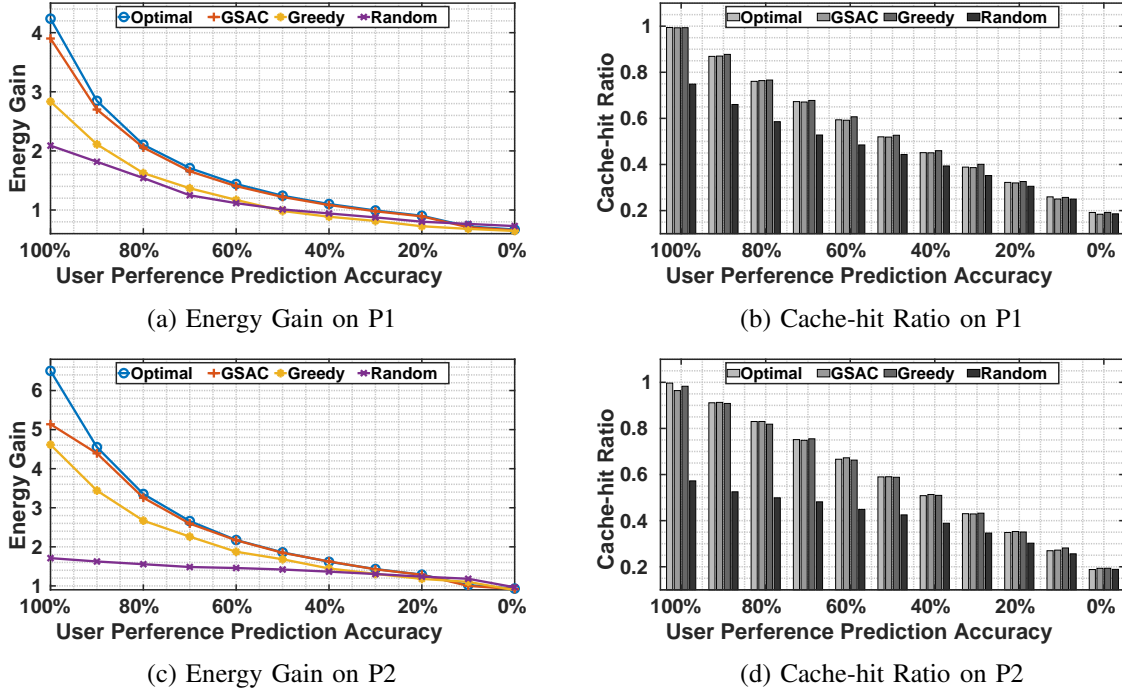


Figure 4: Algorithms Performance versus Preference Prediction Accuracy

V. CONCLUSIONS

To meet the significant growth of popular on-demand content whilst empowering a network energy efficiency operation, we jointly consider the problem of anchoring popular content at network nodes with caching capabilities and deciding delivery routing paths. The proposed integer linear programming model amalgamates energy consumption, the constraints of caching memory, link bandwidth, multipath routing, and different delivery mode, i.e. multicast and unicast. In

addition, a greedy simulated annealing caching algorithm is presented and the effectiveness of the proposed schemes is evaluated by a wide set of numerical investigations. For instance, we test the performance of evaluated algorithms under different network resources, topologies, and user preference predictions. The experimental data suggests that the proposed algorithms reduce the energy consumption up to 60% compared with other caching schemes. Furthermore, expanding link bandwidth, increased path diversity and increasing the preference prediction accuracy have beneficial effects on energy saving. For future work, we plan to consider AI-driven algorithms in the proposed framework to augment the model with learning capabilities so that the optimal allocation patterns can be learnt autonomously.

REFERENCES

- [1] P. Cerwall, P. Jonsson, and S. Carson, "Ericsson mobility report.(november 2018)," *White Paper*, 2018.
- [2] G. Xylomenos, C. N. Ververidis, V. A. Siris, N. Fotiou, C. Tsilopoulos, X. Vasilakos, K. V. Katsaros, and G. C. Polyzos, "A survey of information-centric networking research," *IEEE Communications Surveys & Tutorials*, vol. 16, no. 2, pp. 1024–1049, 2014.
- [3] Y. Wang and V. Friderikos, "A survey of deep learning for data caching in edge network," in *Informatics*, vol. 7, p. 43, Multidisciplinary Digital Publishing Institute, 2020.
- [4] C. Fang, H. Yao, Z. Wang, W. Wu, X. Jin, and F. R. Yu, "A survey of mobile information-centric networking: Research issues and challenges," *IEEE Communications Surveys & Tutorials*, 2018.
- [5] S. Buzzi, I. Chih-Lin, T. E. Klein, H. V. Poor, C. Yang, and A. Zappone, "A survey of energy-efficient techniques for 5g networks and challenges ahead," *IEEE Journal on Selected Areas in Communications*, vol. 34, no. 4, pp. 697–709, 2016.
- [6] N. Choi, K. Guan, D. C. Kilper, and G. Atkinson, "In-network caching effect on optimal energy consumption in content-centric networking," in *Communications (ICC), 2012 IEEE International Conference on*, pp. 2889–2894, IEEE, 2012.
- [7] J. Llorca, A. M. Tulino, K. Guan, J. Esteban, M. Varvello, N. Choi, and D. C. Kilper, "Dynamic in-network caching for energy efficient content delivery," in *INFOCOM, 2013 Proceedings IEEE*, pp. 245–249, IEEE, 2013.
- [8] C. Fang, F. R. Yu, T. Huang, J. Liu, and Y. Liu, "An energy-efficient distributed in-network caching scheme for green content-centric networks," *Computer Networks*, vol. 78, pp. 119–129, 2015.
- [9] F. Dehghani and N. Movahhedinia, "Ccn energy-delay aware cache management using quantized hopfield," *Journal of Network and Systems Management*, pp. 1–21, 2018.
- [10] J. Li, B. Liu, and H. Wu, "Energy-efficient in-network caching for content-centric networking," *IEEE Communications Letters*, vol. 17, no. 4, pp. 797–800, 2013.
- [11] Q. Chen, F. R. Yu, T. Huang, R. Xie, J. Liu, and Y. Liu, "Joint resource allocation for software-defined networking, caching, and computing," *IEEE/ACM Transactions on Networking*, vol. 26, no. 1, pp. 274–287, 2018.
- [12] L. Li, D. Shi, R. Hou, R. Chen, B. Lin, and M. Pan, "Energy-efficient proactive caching for adaptive video streaming via data-driven optimization," *IEEE Internet of Things Journal*, vol. 7, no. 6, pp. 5549–5561, 2020.
- [13] J. Xu, K. Ota, and M. Dong, "Energy efficient hybrid edge caching scheme for tactile internet in 5g," *IEEE Transactions on Green Communications and Networking*, vol. 3, no. 2, pp. 483–493, 2019.
- [14] H. Zhang, Y. Wang, H. Ji, and X. Li, "A sleeping mechanism for cache-enabled small cell networks with energy harvesting function," *IEEE Transactions on Green Communications and Networking*, vol. 4, no. 2, pp. 497–505, 2020.

- [15] Y. Meng, Z. Zhang, and Y. Huang, "Cache-and energy harvesting-enabled d2d cellular network: Modeling, analysis and optimization," *IEEE Transactions on Green Communications and Networking*, 2021.
- [16] F. Zafari, J. Li, K. K. Leung, D. Towsley, and A. Swami, "Optimal energy tradeoff among communication, computation and caching with qoi-guarantee," in *2018 IEEE Global Communications Conference (GLOBECOM)*, pp. 1–7, IEEE, 2018.
- [17] B. Liu, K. Poularakis, L. Tassiulas, and T. Jiang, "Joint caching and routing in congestible networks of arbitrary topology," *IEEE Internet of Things Journal*, vol. 6, no. 6, pp. 10105–10118, 2019.
- [18] W. Chu, M. Dehghan, J. C. Lui, D. Towsley, and Z.-L. Zhang, "Joint cache resource allocation and request routing for in-network caching services," *Computer Networks*, vol. 131, pp. 1–14, 2018.
- [19] S. Ioannidis and E. Yeh, "Jointly optimal routing and caching for arbitrary network topologies," *IEEE Journal on Selected Areas in Communications*, vol. 36, no. 6, pp. 1258–1275, 2018.
- [20] A. Seetharam, "On caching and routing in information-centric networks," *IEEE Communications Magazine*, vol. 56, no. 3, pp. 204–209, 2017.
- [21] D. Liu, B. Chen, C. Yang, and A. F. Molisch, "Caching at the wireless edge: design aspects, challenges, and future directions," *IEEE Communications Magazine*, vol. 54, no. 9, pp. 22–28, 2016.
- [22] O. Ayoub, F. Musumeci, M. Tornatore, and A. Pattavina, "Energy-efficient video-on-demand content caching and distribution in metro area networks," *IEEE Transactions on Green Communications and Networking*, vol. 3, no. 1, pp. 159–169, 2018.
- [23] C. Yang, Z. Chen, B. Xia, and J. Wang, "When icn meets c-ran for hetnets: an sdn approach," *IEEE Communications Magazine*, vol. 53, no. 11, pp. 118–125, 2015.
- [24] Y. Wang, G. Zheng, and V. Friderikos, "Proactive caching in mobile networks with delay guarantees," in *ICC 2019-2019 IEEE International Conference on Communications (ICC)*, pp. 1–6, IEEE, 2019.
- [25] B. Chen and C. Yang, "Caching policy for cache-enabled d2d communications by learning user preference," *IEEE Transactions on Communications*, vol. 66, no. 12, pp. 6586–6601, 2018.
- [26] J. Ren, H. Tian, Y. Lin, S. Fan, G. Nie, H. Wu, and F. Zhang, "Incentivized social-aware proactive device caching with user preference prediction," *IEEE Access*, vol. 7, pp. 136148–136160, 2019.
- [27] M. I. A. Zahed, I. Ahmad, D. Habibi, and Q. V. Phung, "Content caching in industrial iot: Security and energy considerations," *IEEE Internet of Things Journal*, vol. 7, no. 1, pp. 491–504, 2019.